Design, simulation, and testing of a novel micro-channel heat exchanger for natural gas cooling in automotive applications

Y. Deng[1, 2], S. Menon[1], Z. Lavrich[1], H.Wang[3], C.L. Hagen[1*]
[1]*Oregon State University - Cascades, Bend, OR, USA*
[2]*Wuhan University of technology, Wuhan, Hubei, China*
[3]*Oregon State University, Corvallis, OR, USA*

Abstract
Micro-channel heat exchangers offer potential for a highly compact solution in heat transfer applications that have space limitations. Mobile applications such as automotive vehicles are one such area. This work presents the design, modeling, simulation and testing of a two-region micro-channel heat exchanger, employing both engine coolant and R134a, for use in an engine that compresses natural gas for on-board refueling at pressures up to 250 bar. The novel design of the micro-channel heat exchanger is presented. Numerical simulations were performed using ANSYS Fluent utilizing extrapolation techniques to estimate the pressure drop as a function of flow rate and symmetry methods to investigate heat transfer. Pressure drop was determined experimentally, and heat transfer was investigated through system tests employing the novel engine. Experimental results showed good comparison with corresponding numerical simulations which demonstrated the validity of the applied extrapolation and symmetry methods, enabling considerable reduction in computational cost. The pressure drop, flow distribution, and heat transfer characteristics of the heat exchanger are discussed.
Keywords: Micro-channel heat exchanger; Computational fluid dynamics (CFD); Fluid flow; Heat transfer; Natural gas; R-134a

1. Introduction

Natural gas is emerging as a promising alternative to liquid hydrocarbon fuels for transportation applications as a result of production increases from directional drilling and hydraulic fracturing, lower cost than gasoline, reduced reliance on imported oil, and environmental benefits [1]. However, a key challenge to overcome is the lack of refueling infrastructure. To this end, a novel bi-modal engine has been developed that allows on-board refueling of natural gas (NG) [2, 3]. Engine development, implementation and packaging are the focus of current efforts [4]. Utilizing cylinder de-activation, some cylinders of a multi-cylinder internal combustion (IC) engine perform two stages of natural gas compression, while an external engine driven compressor performs an additional third stage compression, all with the engine working near idle speed. The process is being developed with the aim of filling an 11.5 gasoline gallon equivalent (GGE) tank to about 250 bar (3600 psi) in less than an hour using a low pressure (~0.25 psi) residential natural gas supply.

The compression process results in considerable heating, which is undesirable [2, 3, 5] because of increased specific volume necessitating increased work input, potential damage to engine seals and valving, changes in engine performance resulting from fuel pre-heating, and thermal cooking of oil in the gas stream [6]. Micro-channel heat exchanger technologies are emerging as a promising cooling solution offering high performance, compact size and lower pressure drops compared to conventional cooling technologies [7]. A micro-channel heat exchanger test performed by Cetegen [8, 9] demonstrated a heat transfer coefficient of 130,000 W/m^2K using the non-aqueous refrigerant HFE-7100. The decreased dimensions of micro-channels result in more compact heat exchangers and higher heat transfer coefficients as a result of increased surface area per unit volume. Micro-channel heat exchangers may achieve surface area per unit volume as high as 1500 m^2/m^3 [10]. Micro-channels have been successfully applied in automotive air conditioning systems [11],

*Corresponding author. Tel. +1-541-322-2061; E-mail address:chris.hagen@oregonstate.edu

fuel cells [12], and microelectronics [13]. Automobile radiators with channels on the scale of micrometers to millimeters enable the use of less refrigerant without increasing size or weight of the refrigerant system [14]. Further development of micro-channel heat exchanger technology has been motivated by requirements of specific process conditions such as low flow rate and high operating pressures. Conventional plate type heat exchangers are typically rated to maximum pressures of 40 bar [15] and have an average area density of approximately 200 m^2/m^3 [16]. Tests of micro-channels conducted by Wu [17] applied pressures of more than 40 bar. The diffusion-bonding process typically used in the construction of micro-channel heat exchangers allows operating pressures as high as 1000 bar [18]. Therefore, the use of a micro-channel heat exchanger is especially attractive for the 3rd stage cooling in the present application given the stringent volume constraints and high operating pressures (of up to 250 bar).

This work presents details of the heat exchanger design process along with the selected heat sinks, the final configuration, and dimensions. Steady flow tests were conducted to evaluate the pressure drop in the heat exchanger pathways. Numerical simulations of the flow field were conducted using ANSYS FLUENT and findings were correlated with the steady-flow measurements. Air compression tests were carried out on an engine setup utilizing the micro-channel heat exchanger for cooling. Numerical simulations of the heat transfer process were performed and findings from experiments and simulations were correlated.

2. Heat exchanger design

a. Cooling requirements and heat sink configuration

The 3rd stage heat exchanger working requirements are presented in Table 1 [4].

Table 1. Specifications for the 3rd stage micro-channel heat exchanger

	Unit	NG	EC	R134a
Mass flow	g/s	24.4	105	36
Inlet temperature	℃	145	80	9
Outlet temperature	℃	25	90	13
Heat load	kW	9.6	3.8	5.7

Air, engine coolant (EC), and refrigerant (R134a) were considered as heat sinks since they are present onboard the vehicle. Atmospheric air is freely available, but would require a blower onboard the vehicle. Further, the low specific heat capacity of atmospheric air results in a large heat exchanger volume, and is thus not a viable option for this application. EC and R134a are available onboard the vehicle, in the engine cooling and air conditioning (a/c) systems respectively.

EC alone is not capable of cooling natural gas to the required exit temperature because high EC temperature (around 90°C) is required for optimum engine combustion performance [19]. The cooling capacity of the a/c system alone is also less than the total cooling load. An energy flow model indicated that the total cooling capacity available using both the engine coolant and air-conditioning circuits was only slightly less than the total cooling load for natural gas (see Table 1) and engine cylinder heat transfer is expected to make up for this small difference [5].

b. Micro-channel heat exchanger overall design

By utilizing the EC and R134a available onboard the vehicle, it appears possible to have a self-contained system for natural gas cooling employing a two-region micro-channel heat exchanger with EC in the first region and R134a in the second region. Since counter-flow plate heat exchangers with both fluids enclosed within internal passages are generally more compact than parallel flow heat exchangers and size is the biggest constraint driving the current design process, the micro-channel heat exchanger was configured as counter-flow. Fig. 1 depicts the micro-channel heat exchanger discussed in this work.

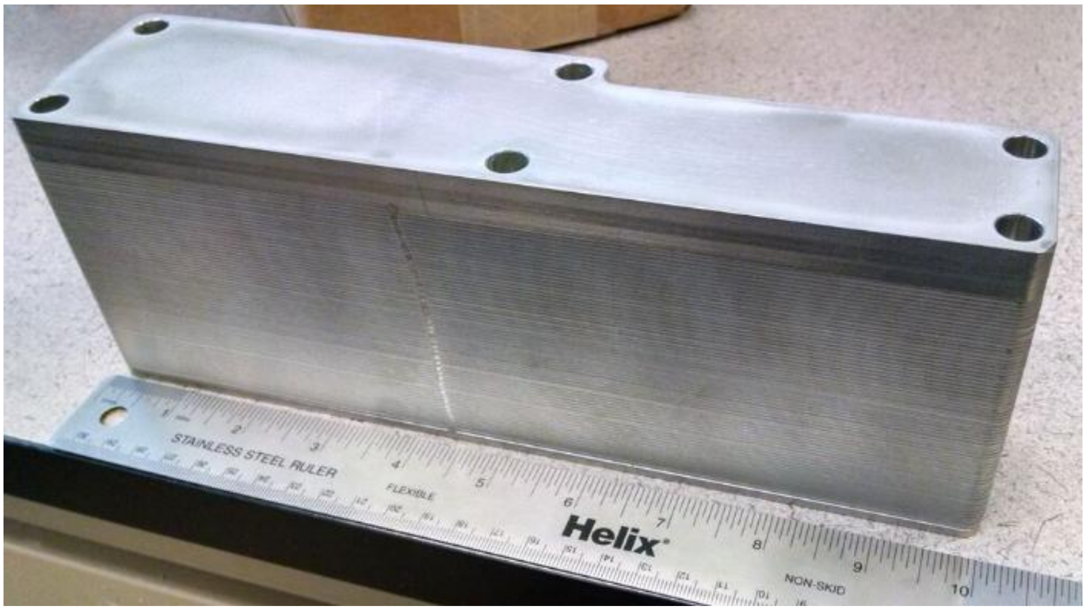

Fig. 1. Overall design of the micro-channel heat exchanger for this work

c. Micro-channel heat exchanger shim design

The micro-channel heat exchanger consists of a bottom plate, cover plate, and 32 pairs of shims. Each pair of shims contains a NG shim and heat sink shim as shown in Fig. 2. Stainless steel was used for its superior anti-corrosion, thermal and mechanical properties.

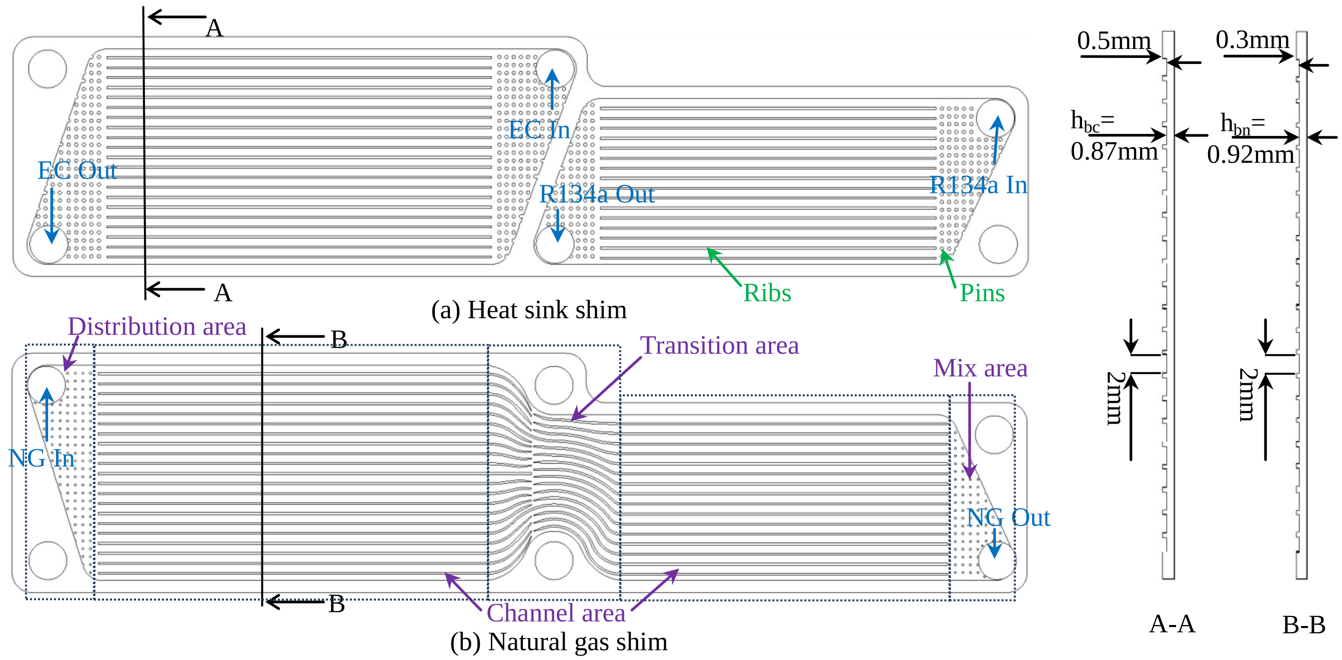

Fig. 2. Shim designs for the micro-channel heat exchanger

A novel shim design as shown in Fig. 2(a) was developed that incorporates flow paths of the two regions into a single heat sink shim. The 1st region accommodates EC flow and the 2nd region provides flow passage for R134a. The R134a and EC channel heights and widths are the same. Fig. 2(b) shows the shim design for natural gas flow. The shims contain 22 channels in the 1st region and 17 channels in the 2nd region. The design dimensions of the micro-channel heat exchanger are shown in Table 2. In this work, the layer closest to the top of the heat exchanger (where the inlet pipes enter the heat exchanger) was defined as the 1st layer, and the channels were numbered starting at the inlet and increasing in the direction of the outlet. The last channel of each region has a smaller width than the other channels.

Table 2. Design dimensions of the micro-channel heat exchanger

		Length(mm)	Width(mm)	Height(mm)
Channel	EC	96.6	2	0.5
	R134a	84.3	2	0.5
	NG	213	2	0.3
Shim	heat sinks	250	60	1.37
	NG	250	60	1.22
Heat exchanger		250	60	98.6

d. Fabrication of the micro-channel heat exchanger

The micro-channel heat exchanger was fabricated in two steps. The individual shims were fabricated using photo-chemical etching for the pin and rib structures followed by laser machining of the through holes and perimeter. The shims, along with the cover plate and bottom plate, were then diffusion bonded in a vacuum furnace under an applied force at high temperature conditions resulting in the final device [20].

e. Actual dimensions of the micro-channel heat exchanger

When the heat exchanger was fabricated from the shim plates the total height of the heat exchanger decreased from 98.6mm to 89.5mm, while the total width of the heat exchanger increased by approximately 0.18-0.83 mm compared to the original specifications. Attempts were made to nondestructively verify the resulting internal geometry, but the diffusion bonded shims do not separate and borescoping and X-ray photographing approaches were not feasible. In this work several assumptions were made to approximate the geometry of the crushed micro-channels: a) transformation was assumed to occur only in the vertical (height) direction, b) transformation was assumed to only impact the height of the channel, not the thickness of the base of the plate (h_{bc} and h_{bn} in Fig. 2) and c) the change in the height of each channel was assumed to be proportional to the total change in the height of the heat exchanger, resulting in a 36% reduction in channel height .

3. Heat exchanger pressure drop experiment and simulation

a. Bench top testing

For the NG and R134a domains, compressed air flowed through a pressure regulator, pressure gauge and an air flow meter, and a digital manometer was used to measure pressure drop (see Table 3 for instrument details). For the EC domain water was pumped through a circuit with a water flow meter, and pressure transducers placed at the inlet and outlet of the heat exchanger were used to measure the pressure drop.

Table 3. Pressure drop test equipment

Device	Manufacturer	Uncertainty	Model number	Max. reading
Pressure transducers	Omega	±2% full scale	PX309-030A5V	30 psi
Manometer	Dwyer	±0.5% full scale	475-7-FM	100 psi
Air Flow meter	King	±6%	7530-1-1-1-2C17	4 cfm
Water Flow meter	EKM	±5%	HOT-SPWM-075	9,999,999.99 cu. ft

b. Simulation setup

ANSYS FLUENT 15.0 [21], was employed to estimate the flow distribution and pressure drop through shims of the micro-channel heat exchanger. A desktop computer with 4 Q9400 2.66GHz processors and total of 8 GB RAM was employed to run the code. To facilitate comparison with the experimental results, the simulated test conditions employed air in the NG and R134a domains, and water in the EC domain. The test conditions thus differed from the design conditions in which engine coolant, R134a and natural gas would flow through the heat exchanger.

Due to the complex structure of each fluid domain it was not practical to build the full size model for simulation, but modeling several layers was feasible. Since each of the fluid domains consist of 32 identical layers, simulations were conducted with increasing numbers of layers (with additional layers added one at a time to the existing layers with the inlet and outlet pipes). A trend line was then generated from the simulation results for the first 6 layers. A linear relationship between pressure drop and flow rate might be expected for laminar flow through the channel areas, however the distribution and mix areas of the heat exchanger, as well as the inlet and outlet pipes, may experience turbulent flow, and other studies of micro-channel heat exchangers have observed a 2nd order polynomial relationship between pressure drop and Reynolds number [22, 23]. A 2nd order polynomial relationship for pressure drop as a function of flow rate, generated from the results of the first 6 simulations, agreed with the results of the simulation for 7 layers, and was thus used to extrapolate to the full 32 layers.

The compressibility of air was neglected, because the velocities were low enough to result in Mach numbers less than 0.3 [24]. Air density, as well as other property values, were assumed to have constant values equal to the average of the values at the inlet and outlet pressures. Gravity was neglected and flow was considered steady state. The standard k-epsilon model and standard wall functions were selected while the channel areas were specified as laminar zones [25, 26]. The wall roughness was set as 2e-05 [27]. The convergence criterion was normalized residuals for mass and momentum conservation of less than 10^{-5}. In order to compare the extrapolated values with the test results, the simulation velocity (v_{sim}) at the pipe inlet was:

$$v_{sim} = \frac{V_{test}}{A*32} * n \tag{1}$$

Where V_{test} is the volume flow rate for the test condition, n is the number of layers, and A is the inlet port area.

c. Results and discussion

i) Overall pressure drop of the heat exchanger

Fig. 3-5 show pressure drop from the inlet to the outlet of each domain. A fit line was assigned to simulations of 1 through 6 shims, and checked against the 7th shim simulation with a maximum error of 0.23% at a flow rate of 0.036 m^3/hr in the EC domain. The fit was then extrapolated to 32 shims. Fig 3 depicts the pressure drop of water flowing through the coolant domain. Extrapolated values are lower than experimental values, with a maximum difference of 3,292 Pa at 0.383 m^3/hr and the maximum percentage error is 25.2% occurring at 0.165 m^3/hr.

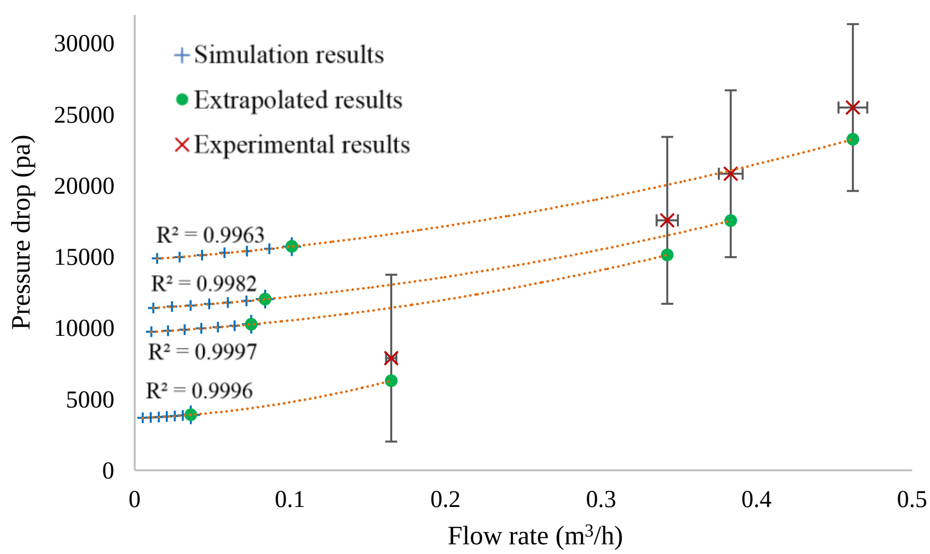

Fig. 3. Pressure drop as a function of flow rate in the coolant domain

A comparison between the values from extrapolation and experiment for the pressure drop of compressed air is shown in Fig. 4 and Fig. 5. The maximum percentage errors are 10.7% and 20% at the lowest test flow rates for the R134a and NG domains respectively.

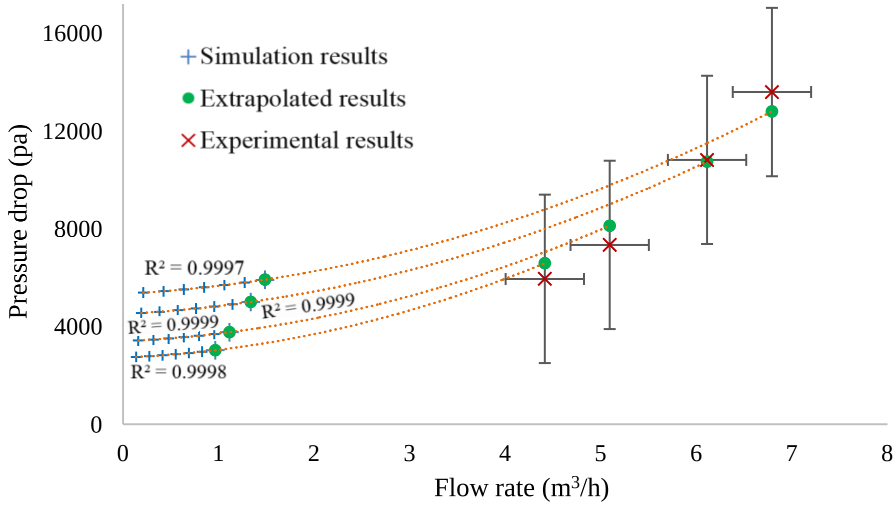

Fig. 4. Pressure drop as a function of flow rate in the R134a domain

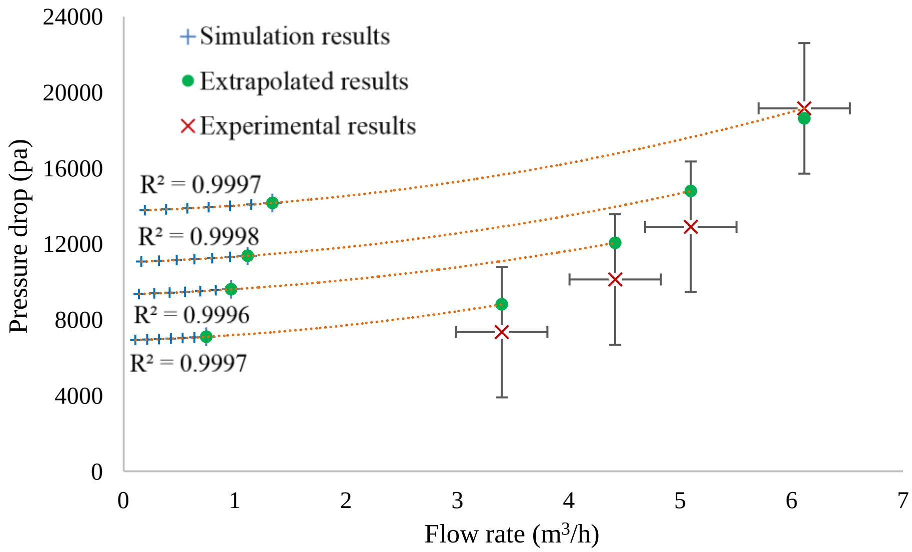

Fig.5. Pressure drop as a function of flow rate in the NG domain

Possible reasons for the difference between experimental and extrapolated values include inexact geometry, errors associated with extrapolation, uncertainty in the sensors, and errors relating to the CFD code. However, the extrapolated values showed reasonable agreement with the experimental values and exhibited similar trends as the experimental values, suggesting that the extrapolation provided a reasonable approximation of the actual values. The pressure drop results depicted in Fig. 3-5 correspond to the test conditions (employing water in the engine coolant domain and air in the natural gas and R134a domains). The pressure drop corresponding to the design conditions (using engine coolant, R134a and natural gas) would differ from the results for the test conditions, particularly for the engine coolant domain as engine coolant is more viscous than water [28].

ii) Pressure drop of the channel area

In order to determine the contribution of the channel area to the total pressure drop of the heat exchanger, pressure drop in the channel area (between the distribution and mix area, see Fig. 2) of a single layer was considered (because the layers are stacked in parallel, each of the layers is expected to experience similar pressure drop). The channel contribution to pressure drop is shown in Fig. 6, which was generated by dividing the pressure drop of the area between the distribution and mix areas determined from the 1 layer simulation, by the extrapolated value for the pressure drop for the entire 32 layers. In Fig. 6 the letters on the x axis correspond to the flow rates at the test conditions as shown in Fig. 3-5 with "a" corresponding to the lowest flow rate and "d" corresponding to the highest flow rate. Over the range of flow rates tested, the channel areas of the EC and R134a domains each made up 7-18% of the total pressure drop, while the area between the distribution and mix area of the NG domain accounted for 45-55% of the total pressure drop. The larger percent pressure drop of the NG domain is likely a result of the transition area (as shown in Fig. 2). As expected, with increasing flow rate, percent pressure drop in the channels decreases, as turbulent conditions in the distribution and mix areas have a larger contribution.

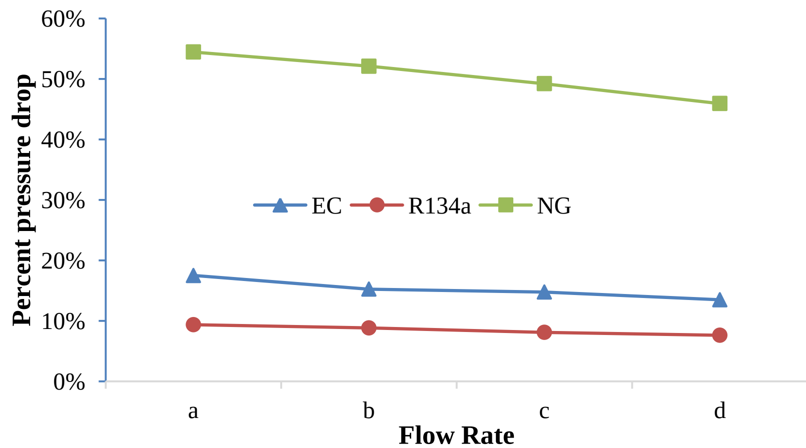

Fig. 6. Channel area percentage of pressure drop

iii) Flow distribution

Flow maldistribution may result in reduced heat transfer and increased pressure drop. Flow maldistribution was first considered by Bassoiuny [29]. Later Rao [30] and Tsai [31] investigated flow maldistribution in plate heat exchangers, while micro-channel heat exchanger flow maldistribution was examined by Vásquez-Alvarez [32]. The dimensionless flow rate of a particular channel or layer (G_i^*) is given by the mass flow rate of the channel or layer ($\mathrm{G_i}$) divided by the total mass flow rate of all of the channels or layers ($\mathrm{G_t}$), such that:

$$G_i^* = \frac{G_i}{G_t} \quad (2)$$

Fig. 7 shows the layer flow distribution of the heat exchanger for the 6 layer simulation. The difference between uneven distributions is less than 0.1%.

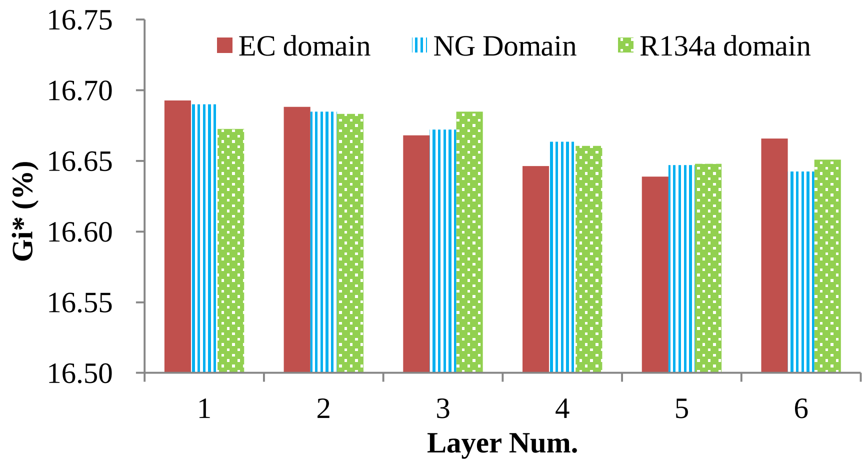

Fig. 7. Flow distribution of each layer for the 6 layer simulation

Fig. 8 shows the channel flow distribution in each region of the 3rd layer of the heat exchanger for the 6 layer simulation. Heat sink channels had a more uniform flow distribution, while the NG domain shows more variation, possibly because of the transition area of the NG shim as compared to the straight and regular channels of the heat sink shim. The 22nd channel in the 1st region and the 17th channel in the 2nd region have the lowest flow rates since they have smaller channel widths and are far from the ports.

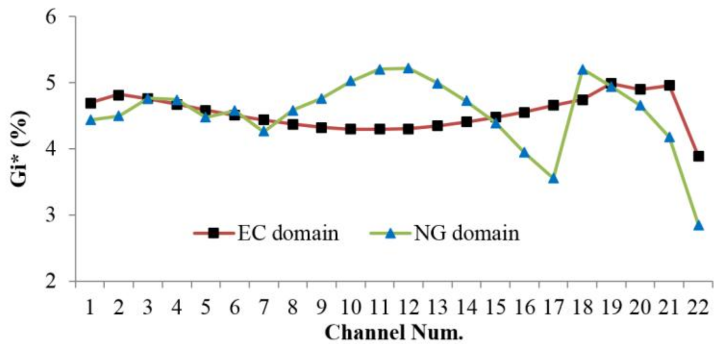

(a) Channel flow distribution in the 1st region

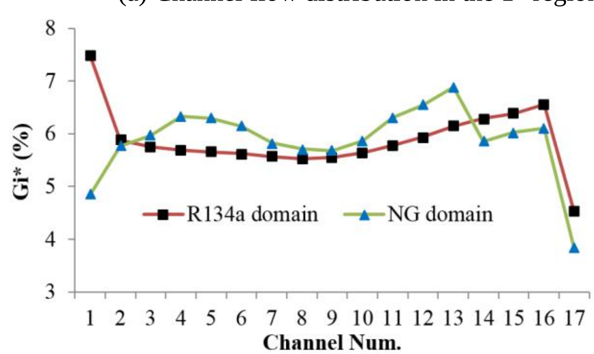

(b) Channel flow distribution in the 2nd region

Fig. 8. Channel flow distribution of the 3rd layer

The flow distribution results presented in Fig 7-8 correspond to the test conditions, not the design conditions of the heat exchanger. Results for the R134a domain are for air while the heat exchanger was designed for two phase flow of R134a. The flow distribution under design conditions would differ from these results for the test conditions [33].

4. Heat exchanger single phase heat transfer experiment and simulations

a. System compression tests

System compression tests were conducted by driving the engine with an external motor. The micro-channel heat exchanger was tested in the second stage heat exchanger position to alleviate overpressure concerns during device characterization. For safety reasons, air was used as the working fluid instead of natural gas. Water was used in place of EC and R134a and flow rates were indicated by flow meters. Thermocouples and pressure transducers were employed to measure air and water inlet and outlet temperatures, as well as air outlet pressure. Air exiting the heat exchanger flowed into a tank where temperature and pressure were measured and used to calculate the mass flow rate of air by application of the ideal gas equation of state.

b. Simulation setup

In the heat exchanger, heat sink and NG domains alternate periodically as shown in Fig. 9(a). The fluid in each layer exhibits flow symmetry about the mid plane, but since the thickness of the solid plates ($h_{bc} \neq h_{bn}$ in Fig. 2 and Fig. 9(a)) differs by 0.05 mm, symmetry does not strictly exist in heat transfer. To reduce the extent of the computational model, a symmetry boundary condition was applied assuming that both plates were the same thickness (the average of h_{bc} and h_{bn}) as shown in Fig. 9(b).

In order to determine the boundary conditions, the difference in geometry of the top and bottom plates (specifically the lack of a heat sink or natural gas channel as compared to layers within the heat exchanger) was neglected, such that the flow rate for the computational domain ($\dot{V}_s$) was given by the flow rate of the heat exchanger from the system compression tests ($\dot{V}_m$) divided by 64, while the inlet temperature of the computational domain (T_s) was given by the measured heat exchanger inlet temperature (T_m), or:

$$\dot{V}_s = \frac{\dot{V}_m}{64} \qquad and \quad T_s = T_m \tag{3}$$

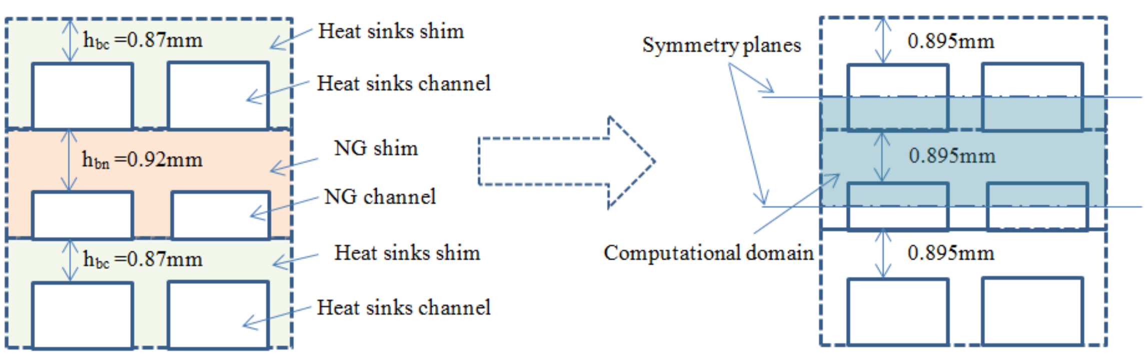

(a) Actual design dimensions (b) Simplified model

Fig. 9. Model of the computational domain

Other assumptions incorporated to simplify the solutions include: 1) steady fluid flow and heat transfer, 2) constant solid and fluid properties, and 3) negligible radiation and natural convection heat transfer.

ANSYS FLUENT was used to simulate the heat transfer of the micro-channel heat exchanger. Simulation results were validated by comparison with the results of system compression tests. The duration of the test was divided into 27 evenly spaced time increments and average values of flow rate and inlet temperature were taken over these time periods for use as inputs to the simulation. The convergence criterion was a residual error of 10^{-8} for energy and 10^{-5} for other residuals.

For the heat transfer simulations the working fluids were air in the NG domain, and water in the EC and R134a domains. The test conditions for the experiments and simulations therefore differed from the design conditions.

c. Results and discussion

Fig. 10 gives air inlet and exit temperatures for the 27 time periods. For the first 400 seconds, only two stages of compression were used, and the mass flow rate, and thus inlet velocity, decreased as the test progressed as a result of the increasing fuel storage tank pressure. After 400 seconds, 3rd stage compression was implemented, and the mass flow rate was closer to constant. The air inlet temperature increased over the first 400 seconds, as a result of heat generated during compression. However, once third stage compression was implemented the inlet air temperature increased only slightly as the test progressed. The simulation and experimental results for outlet air temperature appear to be in good agreement.

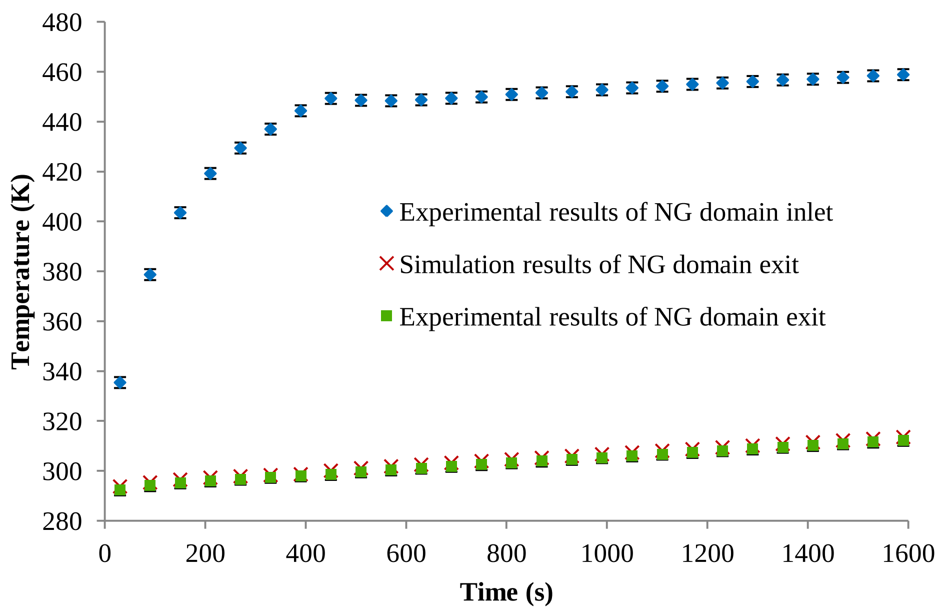

Fig. 10. Inlet and outlet temperatures of air in the NG domain

Fig. 11 illustrates the water inlet and outlet temperatures of the EC domain. By the end of the test, the inlet temperature of water in the EC domain was close to the measured outlet temperature. The water used for cooling was circulated in a closed loop, resulting in an increase in inlet temperature as the test progressed. Other paths of heat transfer may account for the difference between the simulation and experimental results. For example the simulation did not include heat transfer from the walls of the heat exchanger to the surrounding air.

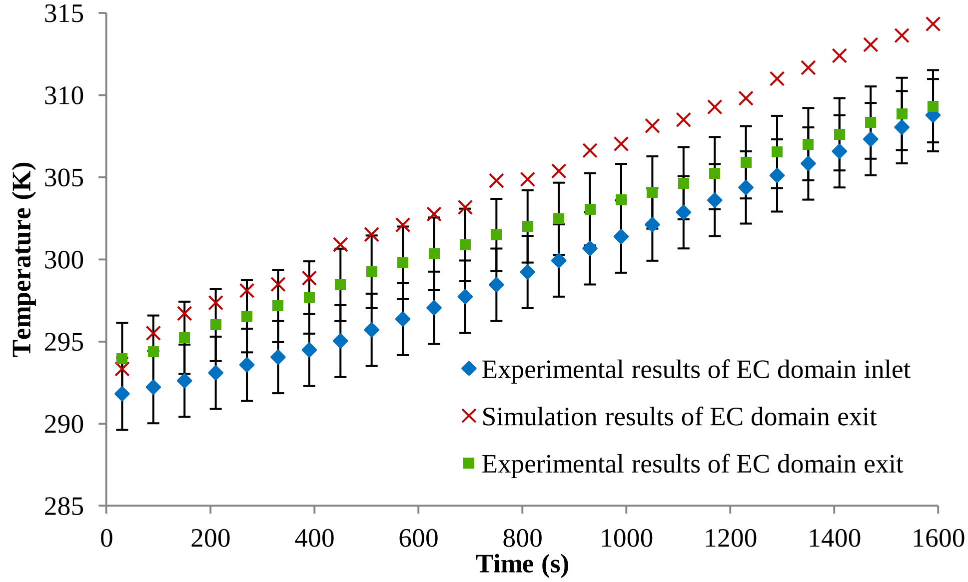

Fig. 11. Inlet and outlet temperatures of water in the EC domain

Fig. 12 depicts the temperature distributions in the solid region as well as the NG, EC and R134a domains. In the solid, large temperature gradients occur in the distribution area near the NG inlet with a maximum temperature difference of about 110℃ indicating a potential for thermal stresses. The fluid temperature distributions indicate cooling of the NG occurred primarily in the distribution area and the channel inlet. Little heat transfer occurred within the channels, suggesting that the heat exchanger did not perform at its design cooling capacity, as might be expected because the test conditions differed from the design conditions. The experimental and simulation results correspond to use of room temperature water as coolant, while the heat exchanger was designed to use engine coolant (at temperatures of about 90 ° C) and R134a.

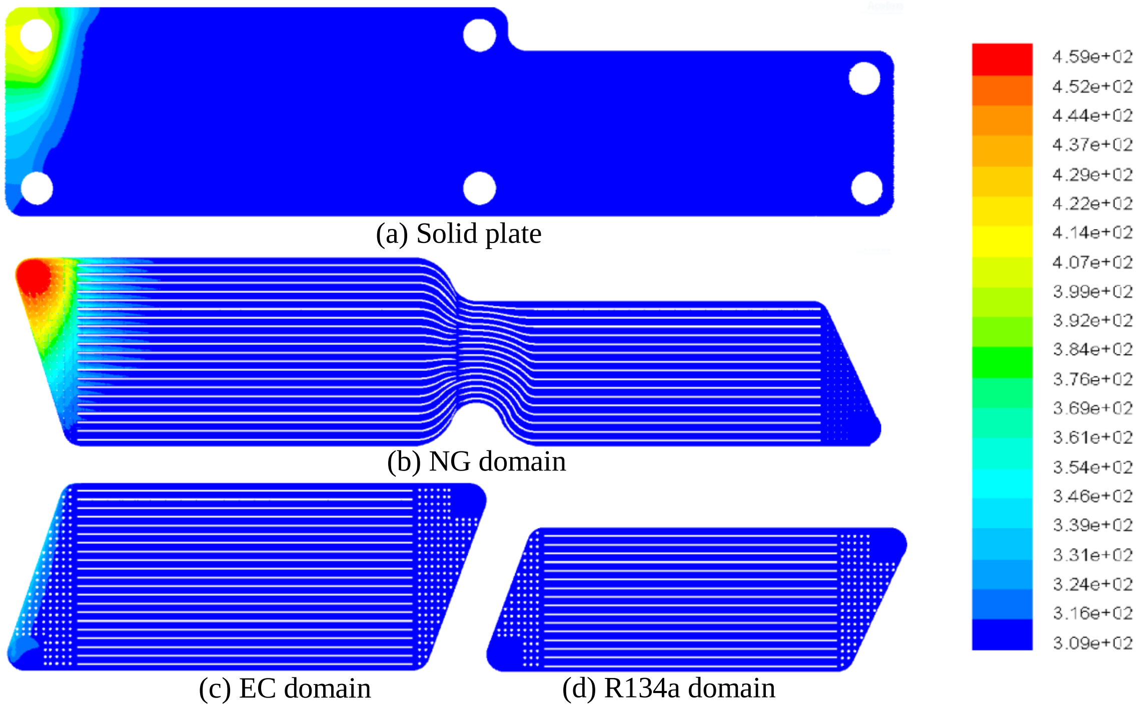

Fig. 12. Temperature distribution of the computational area

5. Conclusion

This work describes the development and evaluation of a novel two-region micro-channel heat exchanger employing engine coolant and R134a for cooling of compressed natural gas on-board a vehicle. The main conclusions from the study are:

a. The extrapolation method provided a satisfactory approximation of the performance of the heat exchanger while saving time and computational resources.
b. The channel area accounts for 7-18% of the total pressure drop for the EC and R134a domains, while the area between the distribution and mix area of the NG domain accounts for 45-55% of the total pressure drop over the range of flow rates considered.
c. The fluid distribution is similar in each layer and the flow is evenly distributed to the channels within a layer.
d. Although heat transfer symmetry may not strictly exist in this case, the geometry of the heat exchanger was determined to be sufficiently close to symmetric to allow for the application of a symmetry boundary condition which greatly reduced the computational load while providing reasonably accurate results.
e. The temperature distribution of the heat exchanger indicates that the majority of the heat transfer occurred only in the distribution area and the channel inlet area of the NG domain, suggesting that the heat exchanger has a higher cooling capacity than required by the test conditions. In addition, thermal stress may have a significant impact on the performance of the micro-channel heat exchanger, as areas near the inlet pipes may experience a much higher temperature than the surrounding areas.

6. Acknowledgments

The information, data, or work presented herein was funded in part by the Advanced Research Projects Agency-Energy (ARPA-E), U.S. Department of Energy, under Award Number DE-AR0000490. The authors are also grateful for the support awarded through OnBoard Dynamics, Inc. from the Oregon nanoscience and microtechnologies institute (ONAMI) and through a gap-grant award and Oregon Built Environment & Sustainable Technologies Center, Inc. (BEST) and collaborative efforts with Czero. Chris Hagen holds equity in Onboard Dynamics, Inc., a company that integrates natural gas compressor technology into automotive engines.

7. Disclaimer

8. References

1. Suurs, R.A.A., Hekkert, M.P., Kieboom S., Smits, R.E.H.M., "Understanding the Formative Stage of Technological Innovation System Development: The Case of Natural Gas as an Automotive Fuel", Energy Policy, Vol. 38, Issue 1, January 2010, pp. 419–431
2. Elgin, R.C., Hagen, C L., "Development and Operation of a Self-Refueling Compressed Natural Gas Vehicle", Applied Energy, Oct 1, 2015, Vol.155, pp. 242-253
3. Echter, N.P., Weyer, K.M., Turner, C.W., Babbitt, G.R., Hagen, C.L., "Design and Analysis of a Self-Refueling CNG Vehicle to Provide Home Refueling", SAE 2014 World Congress, Detroit, Michigan, USA, 2014, Vol. 2014-01-1341.
4. http://www.onboarddynamics.com/, last downloaded 05/05/16.
5. Menon, S., Ganti, H., Wang H., Hagen, C., "Development and Analysis of Micro-Channel Heat Exchangers for Natural Gas Cooling", ASME 2015 13th International Conference on Nanochannels, Microchannels, and Minichannels, San Francisco, California, USA, July 6–9, 2015.
6. Guo, A., Lin, X., Liu, D., Zhang, X., Wang, Z. "Investigation on Shot-Coke-Forming Propensity and Controlling of Coke Morphology During Heavy Oil Coking", Fuel Processing Technology, Volume 104, December 2012, pp. 332–342
7. Khan, M.G., Fartaj, A., "A Review on Micro Channel Heat Exchangers and Potential Applications", International Journal of Energy Research, Vol. 35, Issue 7, 2011, pp. 553-582.
8. Cetegen, E., Baummer, T., Dessiatoun, S., Ohadi, M., "Heat Transfer Analysis of Microgrooved Evaporator and Condenser Surfaces Utilized in a High Heat Flux Two-Phase Flow Loop", ASME International Mechanical Engineering Congress and Exposition, Seattle, 2007.
9. Cetegen, E., Dessiatoun, S., Ohadi, M., "Force Fed Boiling and Condensation for High Heat Flux Applications", 7th Minsk International Seminar "Heat Pipes, Heat Pumps, Refrigerators, Power Sources", Minsk, Belarus, 2008
10. Ohadi, M., Choo, K., Dessiatoun, S., Cetegen, E., "Next Generation Microchannel Heat Exchangers", Springer, 2013.
11. Han, Y., Liu, Y., Li, M., Huang, J., "A Review of Development of Micro-Channel Heat Exchanger Applied in Air-Conditioning System", Energy Procedia, Vol. 14, 2012, pp. 148–153.
12. Tonkovich, A.L.Y., Fitzgerald, S.P., Zilka, J.L., LaMont, M.J., Wang, Y., VanderWiel, D.P., Wegeng, R.S., "Microchannel Chemical Reactors for Fuel Processing Applications. II. Compact Fuel Vaporization", Microreaction Technology: Industrial Prospects, Springer, 2000, pp. 364-371
13. Bharathan, D., Kelly, K., "An Assessment of Air Cooling for Use with Automotive Power Electronics", Thermal and Thermomechanical Phenomena in Electronic Systems, 2008, pp. 37 - 43
14. Checketts, G.T., "Microchannel Radiator: An Investigation of Microchannel Technology with Applications in Automotive Radiator Heat Exchangers", University of North Texas, 2014.

15. Abu-Khader, M.M., “Plate Heat Exchangers: Recent Advances”, Renewable and sustainable energy reviews, Vol. 16, No. 4, 2012, pp 1883-1891.
16. Wadekar, V.V., “Heat Exchangers in Process Industry and Mini-and Micro Scale Heat Transfer”, 5th International Conference on Enhanced, Compact and Ultra-Compact Heat Exchangers: Science, Engineering and Technology, Hoboken, NJ, USA, September 2005.
17. Wu, S., Mai, J., Zohar, Y., Tai, Y.C., Ho, C.M., “A Suspended Microchannel with Integrated Temperature Sensors for High-Pressure Flow Studies”, Micro Electro Mechanical Systems, 1998. MEMS 98. Proceedings, pp. 87-92.
18. Miwa, Y., Noishiki, K., Suzuki, T., Takatsuki, K., “Manufacturing Technology of Diffusion-Bonded Compact Heat Exchanger (DCHE)”, Kobelco technology review, No. 32, December 2013.
19. Khanjani, K., Deng, J., Ordys, A., “Controlling Variable Coolant Temperature in Internal Combustion Engines and Its Effects on Fuel Consumption” SAE/JSAE 2014 Small Engine Technology Conference & Exhibition, November 2014
20. Southall, D., "Diffusion Bonding in Compact Heat Exchangers", Proceedings of 2009 international congress on advances in nuclear power plants, Tokyo, Japan, May 2009
21. FLUENT, ANSYS. "15-Theory Guide, ANSYS." Inc., Canonsburg, PA (2013)
22. Dix, J., Jokar, A., Martinsen, R., “A Microchannel Heat Exchanger for Electronics Cooling Applications”, 6th International Conference on Nanochannels, Microchannels, and Minichannels, Darmstadt, Germany, June 2008
23. Seo, J.W., Kim, Y.H., Kim, D., Choi Y.D, Lee, K.J.,” Heat Transfer and Pressure Drop Characteristics in Straight Microchannel of Printed Circuit Heat Exchangers”, Entropy, Vol. 17, Issue 5, May 2015, pp. 3438-3457
24. White, F.M., Fluid Mechanics, eighth ed., McGraw-Hill Education, New York, New York, 2016, pp. 146
25. Lee, P.S., Garimella, S.V., “Thermally Developing Flow and Heat Transfer in Rectangular Microchannels of Different Aspect Ratios”, International Journal of Heat and Mass Transfer, Vol. 49, Issues 17–18, August 2006, pp. 3060–3067
26. Zhang, J.S., Wang, K., Lu, Y.C., Luo, G.S., “Characterization and Modeling of Micromixing Performance in Micropore Dispersion Reactors”, Chemical Engineering and Processing: Process Intensification, Vol. 49, Issue 7, July 2010, pp. 740–747
27. Çakır, O., “Study of Etch Rate and Surface Roughness in Chemical Etching of Stainless Steel”, Key Engineering Materials, Vol.364-366, 2007, pp. 837-842
28. Bohra, L.K., Flow and Pressure Drop of Highly Viscous Fluids in Small Aperture Orifices, Masters of Science in Mechanical Engineering thesis, Georgia Institute of Technology, June 2004.
29. Bassiouny, M.K., Martin, H. “Flow Distribution and Pressure Drop in Plate Heat Exchangers- I, U-Type Arrangement”, Chemical Engineering Science, Vol. 39, Issue 4, July 1984, pp. 693– 700.
30. Rao, B.P., Das, S.K., “An Experimental Study on the Influence of Flow Maldistribution on the Pressure Drop Across a Plate Exchanger”, Journal of Fluids Engineering, Vol. 126, Issue 4, September 2004, pp. 680 – 691.
31. Tsai, Y.C., Liu, F.B., Shen, P.T., “Investigations of the Pressure Drop and Flow Distribution in a Chevron-Type Plate Heat Exchanger”, International Communications in Heat and Mass Transfer, Vol. 36, Issue 6, July 2009, pp.574-578
32. Vásquez-Alvarez, E., Degasperi, F.T., Morita, L.G., Gongora-Rubio, M.R., Giudici, R., “Development of a Micro-Heat Exchanger with Stacked Plates Using LTCC Technology”, Brazilian Journal of Chemical Engineering, Vol. 27, Issue 3, September 2010, pp. 483-497
33. Dario, E.R., Tadrist, L., Passos, J.C., Review on two-phase flow distribution in parallel channels with macro and micro hydraulic diameters: Main results, analyses, trends, Applied Thermal Engineering, Vol. 59, Issues 1–2, September 2013, pp. 316-335